

# Theabrownin Induces Apoptosis and Tumor Inhibition of Hepatocellular Carcinoma Huh7 Cells Through ASK1-JNK-c-Jun Pathway

This article was published in the following Dove Press journal:  
*OncoTargets and Therapy*

Jiaan Xu<sup>1,2</sup>  
Bo Yan<sup>1,2</sup>  
Lei Zhang<sup>3</sup>  
Li Zhou<sup>2</sup>  
Jin Zhang<sup>4</sup>  
Wenhua Yu<sup>5</sup>  
Xiaoqiao Dong<sup>5</sup>  
Li Yao<sup>1</sup>  
Letian Shan<sup>2</sup>

<sup>1</sup>College of Pharmaceutical Sciences, Zhejiang Chinese Medical University, Hangzhou, People's Republic of China; <sup>2</sup>The First Affiliated Hospital, Zhejiang Chinese Medical University, Hangzhou, People's Republic of China; <sup>3</sup>School of Biological and Chemical Engineering, Zhejiang University of Science and Technology, Hangzhou, People's Republic of China; <sup>4</sup>Theabio Co., Ltd, Hangzhou, People's Republic of China; <sup>5</sup>Department of Neurosurgery, Affiliated Hangzhou First People's Hospital, Zhejiang University School of Medicine, Hangzhou, People's Republic of China

**Purpose:** Theabrownin (TB), a main pigment and bioactive component of tea, has been shown anti-tumor activities against carcinomas, but its effects on hepatocellular carcinoma (HCC) remain unclear.

**Methods:** Hepatocellular carcinoma Huh7 cells were used for analyses. Cell viability assay was performed to determine TB's anti-proliferative effect, and flow cytometry with annexin V-FITC/PI double staining and DAPI staining were performed to determine its pro-apoptotic effect. Real-time PCR and Western blot assays were conducted to detect the molecular actions of TB. And a xenograft model of zebrafishes was established to evaluate the in vivo effect of TB. SP600125 (JNK inhibitor) was in vivo and in vitro used to verify the regulatory role of the JNK signaling pathway in the anti-hepatic carcinoma mechanism of TB.

**Results:** TB exerted significant anti-proliferative and pro-apoptotic effects on Huh7 cells in a dose-dependent manner. The molecular data showed that TB up-regulated the gene expressions of *NOXA*, *PUMA*, *P21*, *Bax*, and *Bim* and up-regulated the protein expressions of ASK-1, Bax, phosphorylated JNK, and phosphorylated c-Jun with down-regulation of Bcl-2. The in vivo data showed that TB exerted significant tumor-inhibitory effect which was even stronger than that of cis-platinum. Furthermore, the JNK inhibitor significantly weakened TB's effects both in vivo and in vitro and blocked the related molecular pathway.

**Conclusion:** TB exerts anti-proliferative, pro-apoptotic, and tumor-inhibitory effects on Huh7 cells through activation of the JNK signaling pathway. For the first time, this study provides new evidence of anti-HCC effects and mechanism of TB.

**Keywords:** hepatocellular carcinoma, theabrownin, apoptosis, JNK, zebrafish

## Introduction

Liver cancer, a common malignancy worldwide, is the second and sixth leading cause of cancer death in males and females, respectively.<sup>1</sup> The five-year relative survival rate for liver cancer is 18.1%, which is second only to pancreatic cancer (8.5%).<sup>2</sup> Hepatocellular carcinoma (HCC) accounts for about 90% of all primary liver cancers, with more than 800,000 new cases annually.<sup>3</sup> HCC has a high incidence in Asia and Africa, due to the prevalence of chronic hepatitis B virus.<sup>1</sup> Besides, there are many other risk factors for HCC, such as hepatitis C virus, aflatoxin exposure, alcohol-related cirrhosis, obesity, type 2 diabetes, and smoking.<sup>4</sup> The mortality rate of HCC is extremely high and almost equal to the incidence rate in most countries.<sup>5</sup> Current therapeutic strategies for HCC include chemo-radiotherapy, surgery, local ablation,

Correspondence: Letian Shan; Li Yao  
Email letian.shan@zcmu.edu.cn;  
yaoli@zcmu.edu.cn

and transcatheter therapy.<sup>6</sup> However, their clinical efficacies are unsatisfactory due to the drug resistance and high recurrence rate, especially when most HCC cases were diagnosed at advanced stages, leading to a tough challenge for the therapy of HCC.<sup>7,8</sup> Therefore, new drug candidates need to be explored and developed for effective treatment of anti-HCC.

Natural products, including Chinese herbal medicines (CHM), have a long history in treating various diseases with good efficacies and low side effects, which have attracted increasing attention in recent decades.<sup>9</sup> As one of the most worldwide consumed natural products, tea has been recorded as a herbal remedy of CHM by the earliest national pharmacopeia “Xin Xiu Ben Cao” (Newly Revised Materia Medica) in Tang Dynasty of China (AD 659). Previous researches showed that tea possessed a variety of health-care effects, such as anti-hyperlipidemia, anti-hypercholesterolemia, anti-obesity, and anti-oxidation.<sup>10,11</sup> Moreover, a prospective cohort study on 8552 individuals concluded that consuming over ten cups of tea per day could decrease the cancer onset in both males and females, indicating an anti-cancer potential of tea.<sup>12</sup> Theabrownin (TB) is the main pigment and bioactive component of tea, which is produced by oxidation and polymerization of tea polyphenols.<sup>13</sup> It has been reported to possess anti-hyperlipidemia, and anti-hypercholesterolemia activities.<sup>14,15</sup> Recently, our previous studies have reported that TB could induce apoptosis and inhibit tumor growth of human lung carcinoma cells, indicating an anti-cancer potential of TB.<sup>16,17</sup>

Up to our knowledge, whether TB is effective in treating HCC remains unknown. To address this issue, this study applied HCC cell line (Huh7) to conduct *in vitro* and *in vivo* assays. A xenograft model of larval zebrafishes was employed for the *in vivo* assay, and a signaling pathway-related mechanism of TB was investigated. This is the first study regarding the anti-HCC effect and mechanism of TB, providing a promising candidate for anti-HCC treatment.

## Materials and Methods

### Chemicals and Reagents

Theabrownin (>90% of purity) was obtained from Theabio Co., Ltd (Hangzhou, China) (Batch number: 20181210002). SP600125 (JNK inhibitor) was purchased from MedChemExpress (Shanghai, China). Dulbecco's modified eagle medium (DMEM) and 0.25% trypsin were purchased from Thermo Fisher Scientific (MA,

USA). Fetal bovine serum (FBS) was purchased from CellMax (Beijing, China). 3-(4,5-Dimethylthiazol-2-yl)-2,5-diphenyltetrazolium bromide (MTT) and dimethyl sulfoxide (DMSO) were obtained from Sigma-Aldrich (Taufkirchen, Germany). ProLong<sup>®</sup> Diamond Antifade Mountant with DAPI was purchased from Invitrogen (CA, USA). Annexin-V: FITC apoptosis detection kit was purchased from BD Biosciences (NJ, USA). TRIZol reagent and real-time polymerase chain reaction (real-time PCR) kits were purchased from TaKaRa Biotechnology Co. Ltd. (Dalian, China). All antibodies were purchased from Cell Signaling Technology Inc. (MA, USA).

### Cell Line and Culture

The human HCC Huh7, HepG2, SK-Hep-1 cell lines were obtained from Shanghai Cell Bank of Chinese Academy of Sciences (Shanghai, China). Huh7, HepG2, and SK-Hep-1 cells were cultured in DMEM containing 10% FBS at 37°C in a humidified 5% CO<sub>2</sub> incubator. The medium was daily changed and the cells were treated with TB in their logarithmic growth phase.

### Zabrafishes

Wild-type AB strain of zebrafishes were obtained from the China Zebrafish Resource Center, Institute of Hydrobiology, China Academy of Science (Wuhan, China) and accredited by the Association for Assessment and Accreditation of Laboratory Animal Care International (SYXK 2012–0171). Larval zebrafishes (2 dpf, days post-fertilization) were obtained by natural pair-mating and housed in a light-controlled aquaculture facility with a standard 14:10 h day/night photoperiod and fed with live brine shrimp twice a day and fry flakes once a day.

### Cell Viability Assay

Cell viability of cells (Huh7, HepG2, and SK-Hep-1) with TB treatment was determined by MTT assay. Cells were seeded on 96-well plates with a density of  $8 \times 10^3$  cells/well in 200  $\mu$ L medium overnight and then treated with TB at various concentrations (0, 50, 100, 200, 300, 500, 600  $\mu$ g/mL) for 24 h and 48 h (only for Huh7 cells). Twenty microliter MTT solution (5.0 mg/mL) was added to each well and the plate was incubated at 37°C for 4 h. After the solution was pipetted off, 100  $\mu$ L DMSO was added to each well to dissolve the formazan crystals. Then the optical density (OD) value was measured at 490 nm with a microplate reader (Biorad Laboratories, Inc., CA, USA). Inhibitory rate (%) =  $[1 - (\text{TB-treated OD} / \text{untreated OD})] \times$

100%. The low, medium, high doses of TB were determined as 100 µg/mL, 200 µg/mL, and 300 µg/mL for further use.

## Cell Morphology and DAPI Staining

Cell apoptosis of Huh7 cells induced by TB was determined by DAPI staining. Cells were seeded on 24-well with a density of  $5 \times 10^4$  cells/well and treated with TB at low, medium, high concentrations for 24 h. Cells were fixed with 4% paraformaldehyde in PBS for 30 min at room temperature, followed by permeabilization with 0.25% Triton X-100 in PBS for 30 min and stained with DAPI for 4 min in dark. The unstained and stained cells were observed under a fluorescence microscope (Carl Zeiss, Göttingen, Germany). Five coverslips were used as replicates of each group and the apoptotic nuclei of cells were visualized.

## Flow Cytometry

Cell apoptosis of Huh7 cells induced by TB was also determined by Annexin-V/PI staining-based flow cytometry. Cells were seeded on 6-well plates with a density of  $3 \times 10^5$  cells/well overnight and then treated with TB at low, medium, high concentrations for 24h. The cells were harvested and washed twice with cold PBS, and then labeled with FITC Annexin V and PI in binding buffer. Fluorescence intensity of the cells was detected by a flow cytometry (BD Biosciences, CA, USA).

## Real-Time PCR (qPCR) Assay

Relative mRNA expressions of targeted genes in Huh7 cells were detected by qPCR assay on an ABI QuantStudio™ 7 Flex Real-Time PCR System (Applied Biosystems, CA, USA). The total RNA of the treated Huh7 cells was extracted by using TRIzol reagent and the RNA concentration was measured by NanoDrop2000 spectrophotometer (Thermo Fisher Scientific, USA). Reverse transcription was subsequently conducted by using Primescript RT master

mix (TaKaRa, Japan) to produce cDNA. According to the instructions, the final PCR reaction system was 20 µL, comprising 0.4 µL PCR Forward Primer, 0.4 µL PCR Reverse Primer, 1 µL template cDNA, 8.2 µL ddH<sub>2</sub>O and 10 µL SYBR® Premix Ex Taq II (Tli RnaseH Plus). The qPCR reaction conditions were as follows: 95°C for 5 min for initial denaturation, followed by 40 cycles of denaturation at 95°C for 10 sec, annealing and extension at 60°C for 30 sec. At the end of each reaction, melting curve analysis was performed. β-Actin was used as the reference gene and the  $2^{-\Delta\Delta CT}$  method was used to analyze the relative mRNA expressions (Table 1).

## Western Blot (WB) Analysis

The treated Huh7 cells were lysed in ice-cold extract buffer (50 mM Tris-HCl, pH 7.4, 150 mM NaCl, 1 mM EDTA, 1% Triton, 0.1% SDS, 5 µg/mL leupeptin, and 1 mM PMSF) containing proteinase inhibitor cocktail (Bimake, Houston, TX, USA). Cells were scraped and transferred into pre-cooled microcentrifuge tubes and vibrated for 30 min at 4°C, followed by centrifugation at 12,000× g for 20 min at 4°C. Then the concentrations of supernatant protein were determined using a BCA protein assay kit (Thermo Fisher Scientific, USA). The proteins were separated by denaturing sodium dodecyl sulfate polyacrylamide gel electrophoresis (SDS-PAGE; 8–12%) and transferred onto a nitrocellulose membrane (Sartorius Stedim, Göttingen, Germany). The membrane was blocked with 5% non-fat milk at 4°C for 2 h, followed by overnight incubation at 4°C with the following primary antibodies: actin, ASK1, JNK, phosphor-JNK, c-Jun, phosphor-c-Jun (Ser63), phosphor-c-Jun (Ser73), Bax, Bcl-2. Following incubation with secondary antibody for 2 h at 4°C, the proteins were incubated for 1 min with Western Lightning® Plus ECL (Perkin Elmer, Inc., Waltham, MA, USA). And the results were visualized using X-ray film (Kodak, Tokyo, Japan).

**Table 1** Primer Sequences Used for qPCR Analysis

Gene	Forward Primer	Reverse Primer
<i>β-actin</i>	5'-CCCGCGAGTACAACCTTCT-3'	5'-CGTCATCCATGGCGAACT-3'
<i>NOXA</i>	5'-GGTCCCTAATCATGGACTCCC-3'	5'-CTGTTTGCCAACTTGCTCCAC-3'
<i>PUMA</i>	5'-GACCTCAACGCACAGTACGAG-3'	5'-AGGAGTCCCATGATGAGATTGT -3'
<i>P21</i>	5'-GGCAGACCAGCATGACAGATT-3'	5'-GCGGATTAGGGCTTCTCT-3'
<i>Bax</i>	5'-CCTTTTCTACTTTGCCAGCAAAC-3'	5'-GAGGCCGTCCCAACCAC-3'
<i>Bim</i>	5'-ACCAAACCAAAGCCGTATCA-3'	5'-GGAGCCAGTAAACGTATTGGAAG-3'

## Animal Experiment in Larval Zebrafishes

According to the manufacturer's protocol, Huh7 cells were stained with CM-Dil (red fluorescence) at a 1:1000 dilution and microinjected into the yolk sac of larval zebrafishes (2 dpf) at a dose of 200 cells/fish to establish the HCC xenograft model. After 24 h of tumor growth, all treated zebrafishes were observed under a fluorescence microscope (AZ100, Nikon, Tokyo, Japan) for model verification. HCC xenograft larval zebrafishes (3 dpf) were divided into several groups (30 fishes each) and cultured in 3 mL fresh fish water in 6-well plates. According to our previous study, the NOAEL (no-observed-adverse-effect-level) of TB and cis-platinum were 16.7  $\mu\text{g}/\text{mL}$  and 15.0  $\mu\text{g}/\text{mL}$ , respectively.<sup>18</sup> Therefore, TB powders and cis-platinum were dissolved into the wells at their NOAEL. SP600125 was dissolved in DMSO to a concentration of 20  $\mu\text{M}$  and diluted to 20 pM by 0.9% saline for intravenous injection. After 24 h treatment, zebrafishes were observed under a fluorescence microscope. The fluorescence intensity (FI) of Huh7-developed tumor mass of zebrafishes was detected and the inhibitory rate was calculated as: Inhibitory rate (%) =  $[1 - (\text{TB treated FI} / \text{untreated FI})] \times 100\%$ .

## Statistical Analysis

Data were expressed as the mean  $\pm$  standard deviation (SD). Data from different groups were compared using one-way ANOVA followed by Fisher's least significant difference (LSD) comparison. A p-value  $< 0.05$  was considered to indicate a significant difference and p-value  $< 0.01$  considered to indicate a very significant difference.

## Results

### Anti-Proliferative Effect of TB

MTT assays and morphological observation were performed to evaluate the anti-proliferation effect of TB on HCC cells. As shown in Figure 1A, TB obviously inhibited the cell viability of Huh7, HepG2 and SK-Hep-1 from 100  $\mu\text{g}/\text{mL}$  to higher doses, and the effects on each cell line were similar at doses above 500  $\mu\text{g}/\text{mL}$ . Then Huh7 cells were treated with TB for 24 h and 48 h. As shown in Figure 1B, TB obviously inhibited the cell viability of Huh7 in a dose- and time-dependent manner. TB at 100, 200 and 300  $\mu\text{g}/\text{mL}$  were used as TB-L, TB-M and TB-H doses for the subsequent experiments. As shown in Figure 1C, after the TB treatment for 24 h, the morphology of Huh7 cells was changed and the detached cells (round

and shrunken shape) were obviously increased with the increasing doses of TB.

### Apoptosis-Inducing Effect of TB

DAPI staining and flow cytometry were performed to evaluate the pro-apoptotic effect of TB on Huh7 cells. As shown in Figure 2A, typical apoptotic cells with chromatin condensation, karyopyknosis and apoptotic bodies (indicated by arrows) were increasingly observed with TB treatment from low to high doses. As shown in Figure 2B, the apoptotic rate (early and late) was obviously increased with the increasing doses of TB, suggesting that TB induced apoptosis on Huh7 cells in a dose-dependent manner.

### Modulation on mRNA Expression by TB

The relative mRNA expression of targeted genes was determined by qPCR assay. As shown in Figure 3, TB significantly up-regulated the expression of *PUMA*, *P21*, *Bax*, and *Bim* mRNA transcripts in Huh7 cells when compared with the control group (each  $P < 0.01$ ). Moreover, TB slightly up-regulated the expression of *NOXA* ( $P > 0.05$ ).

### Modulation on Protein Expression by TB

The protein expression of targeted molecules was determined by WB. As shown in Figure 4, TB significantly up-regulated the expression of ASK1, phosphorylated JNK (p-JNK), phosphorylated c-Jun (p-c-Jun) (Ser 63 and Ser 73), and Bax and down-regulated the expression of Bcl-2 ( $P < 0.01$ ), when compared with the control group (each  $P < 0.05$  or  $P < 0.01$ ).

### Anti-HCC Effect of TB in vivo

As shown in Figure 5, the xenograft model of HCC was successfully established in larval zebrafishes. Compared with the model group, TB significantly inhibited HCC tumor growth with an inhibitory rate of 48.1% ( $P < 0.01$ ). The anti-HCC effect of TB at NOAEL (16.7  $\mu\text{g}/\text{mL}$ ) was even stronger than that of cis-platinum at NOAEL (15  $\mu\text{g}/\text{mL}$ ).

### Verification of the Role of JNK Signaling in the Anti-HCC Effects of TB

SP600125 was used to verify the regulatory role of the JNK signaling pathway in TB-induced tumor inhibition and apoptosis of Huh7 cells. As shown in Figure 6

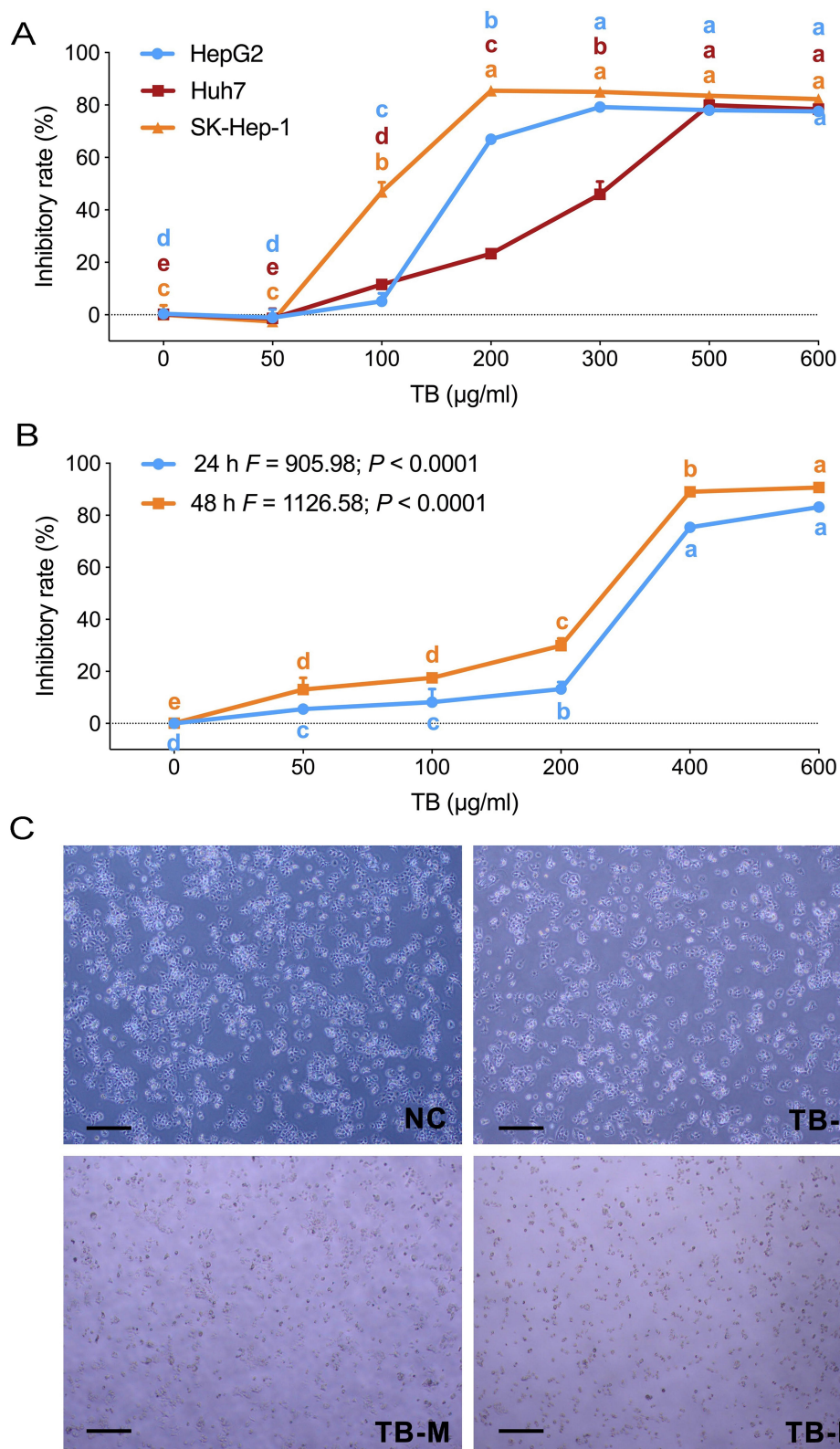


**Figure 1 (A)** Cell viability of HepG2, SK-hepI, and Huh7 cells with TB treatment for 24 h. **(B)** Cell viability of Huh7 cells with TB treatment for 24 and 48 h. **(C)** Morphological observation (light microscope) of Huh7 cells with TB treatment for 24h. Scale bar: 200 µm. Values were presented as the mean ± SD (n = 5). Different symbols (a, ab, b, c, bc, d) indicate significant difference among groups [Fisher's least significant difference (LSD), P < 0.05], and the values decrease with the order from a to d. **Abbreviations:** TB, theabrownin; NC, normal control; TB-L, low dose of theabrownin; TB-M, medium dose of theabrownin; TB-H, high dose of theabrownin.

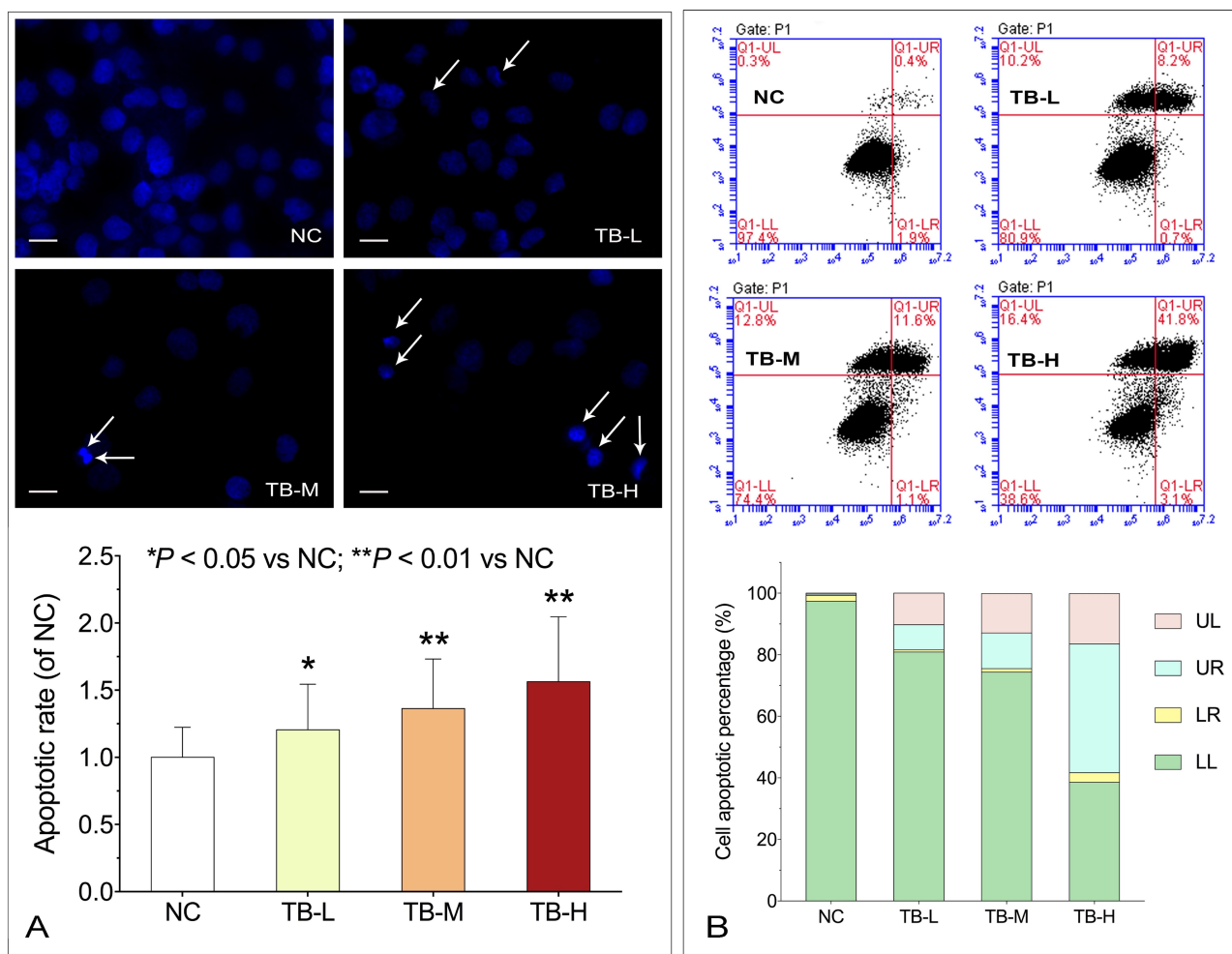


**Figure 2 (A)** Apoptotic morphology of Huh7 cells with TB treatment by DAPI staining. Scale bar: 50  $\mu$ m. Values were presented as the mean  $\pm$  SD (n = 5). \*P < 0.05 and \*\*P < 0.01 vs normal control. **(B)** Flow cytometry analysis on Huh7 cell apoptosis with TB treatment. **Abbreviations:** TB, theabrownin; DAPI, 4',6-diamidino-2-phenylindole; NC, normal control; TB-L, low dose of theabrownin; TB-M, medium dose of theabrownin; TB-H, high dose of theabrownin; UL, upper left quadrant; UR, upper right quadrant; LR, lower right quadrant; LL, lower left quadrant.

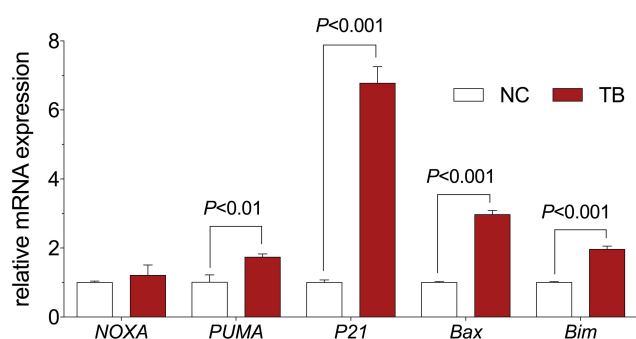


**Figure 3** Relative mRNA expression of target genes in Huh7 cells with TB treatment. Values are presented as mean  $\pm$  SD (n = 3). **Abbreviations:** NC, normal control; TB, theabrownin.

A and B, SP600125 at 20  $\mu$ M significantly weakened the tumor-inhibitory effect of TB in vivo (P < 0.01), and the tumor inhibitory rate was decreased from 44.57% to 26.59%. As shown in Figure 6C, SP600125 at 20  $\mu$ M

significantly relieved TB-induced apoptosis of Huh7 cells, with significant decrease of apoptotic rate (P < 0.01). As shown in Figure 6D, WB data showed that SP600125 significantly inhibited the expression of JNK, p-JNK, c-Jun, and p-c-Jun and meanwhile significantly blocked the regulatory effects of TB on those proteins as well as on the apoptotic proteins (Bax and Bcl-2) (each P < 0.05 or P < 0.01). The above results showed that the JNK signaling mediated TB's effects.

## Discussion

Previous reports have demonstrated that TB possesses hepatoprotective activity against hepatic steatosis and liver damage.<sup>19,20</sup> To date, there is no available report regarding the effect of TB on liver cancer. For the first time, this study revealed pro-apoptotic and tumor-

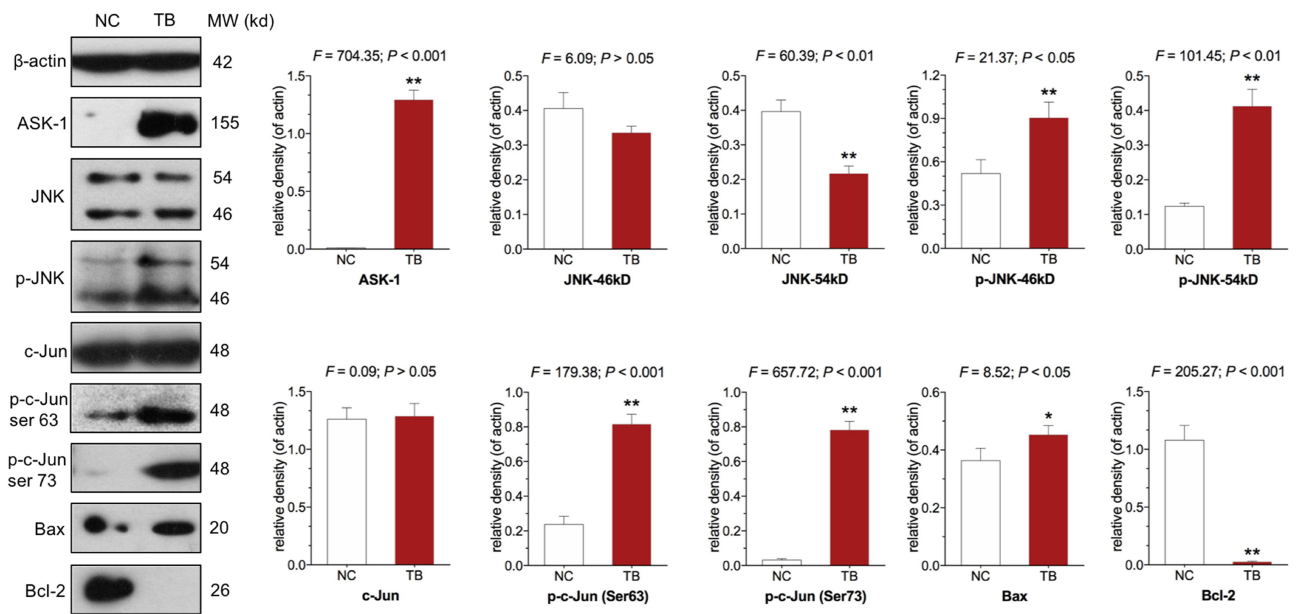


**Figure 4** Expression and phosphorylation of targeted proteins in Huh7 cells with TB treatment. Values represent mean  $\pm$  SD (n = 3). \*P < 0.05 and \*\*P < 0.01 vs normal control. **Abbreviations:** NC, normal control; TB, theabrownin; ASK-1, apoptosis signal-regulating kinase I; JNK, c-Jun N-terminal kinase.

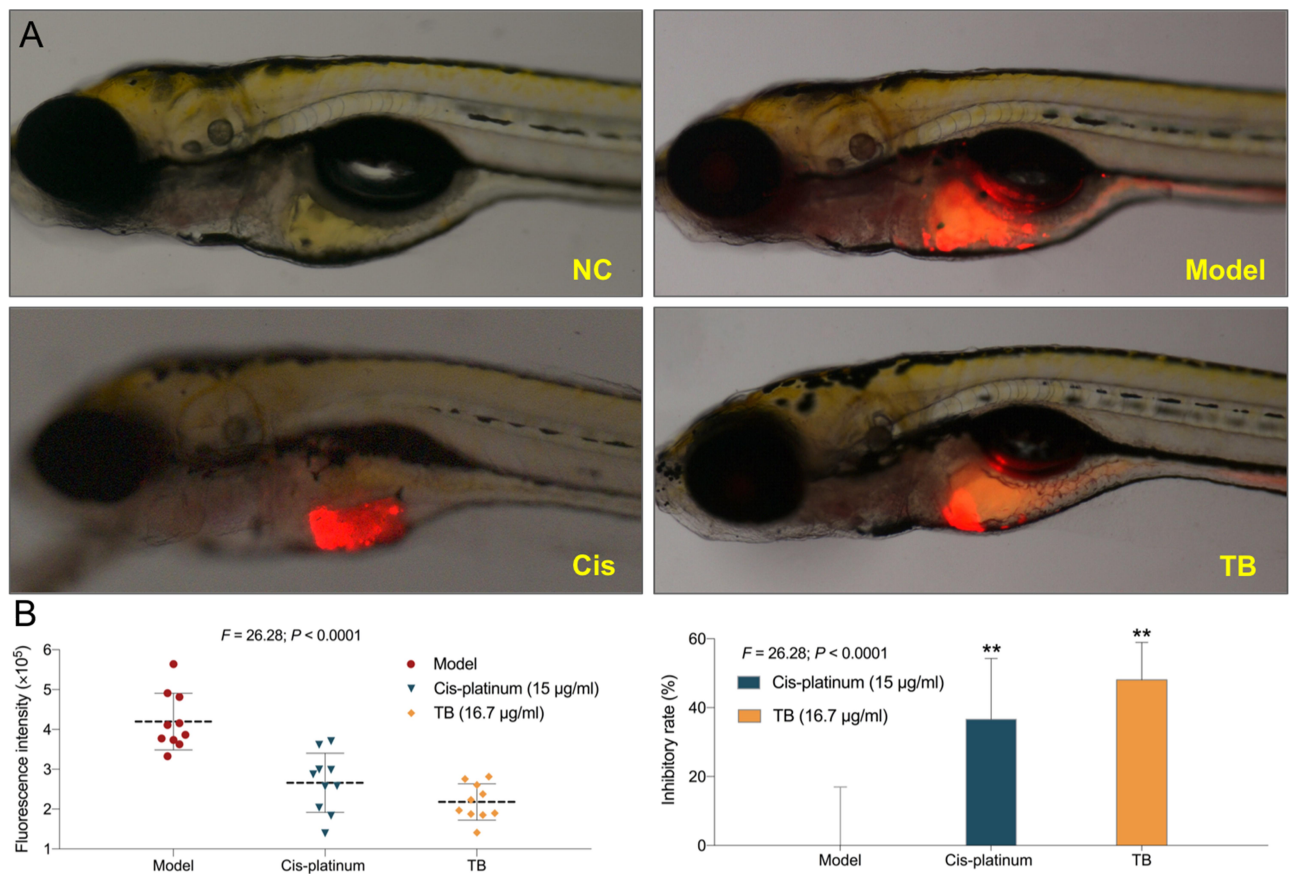


**Figure 5 (A)** Observation of Huh7 xenograft zebrafishes upon treatment with TB or cis-platinum. **(B)** Data of fluorescence intensity and inhibitory effect of TB or cis-platinum. The fluorescent area (red) represents the HCC tumor mass. Values were presented as the mean  $\pm$  SD (n = 30). \*\*P < 0.01 vs model. **Abbreviations:** NC, normal control; TB, theabrownin; Cis, cis-platinum; HCC, hepatocellular carcinoma.

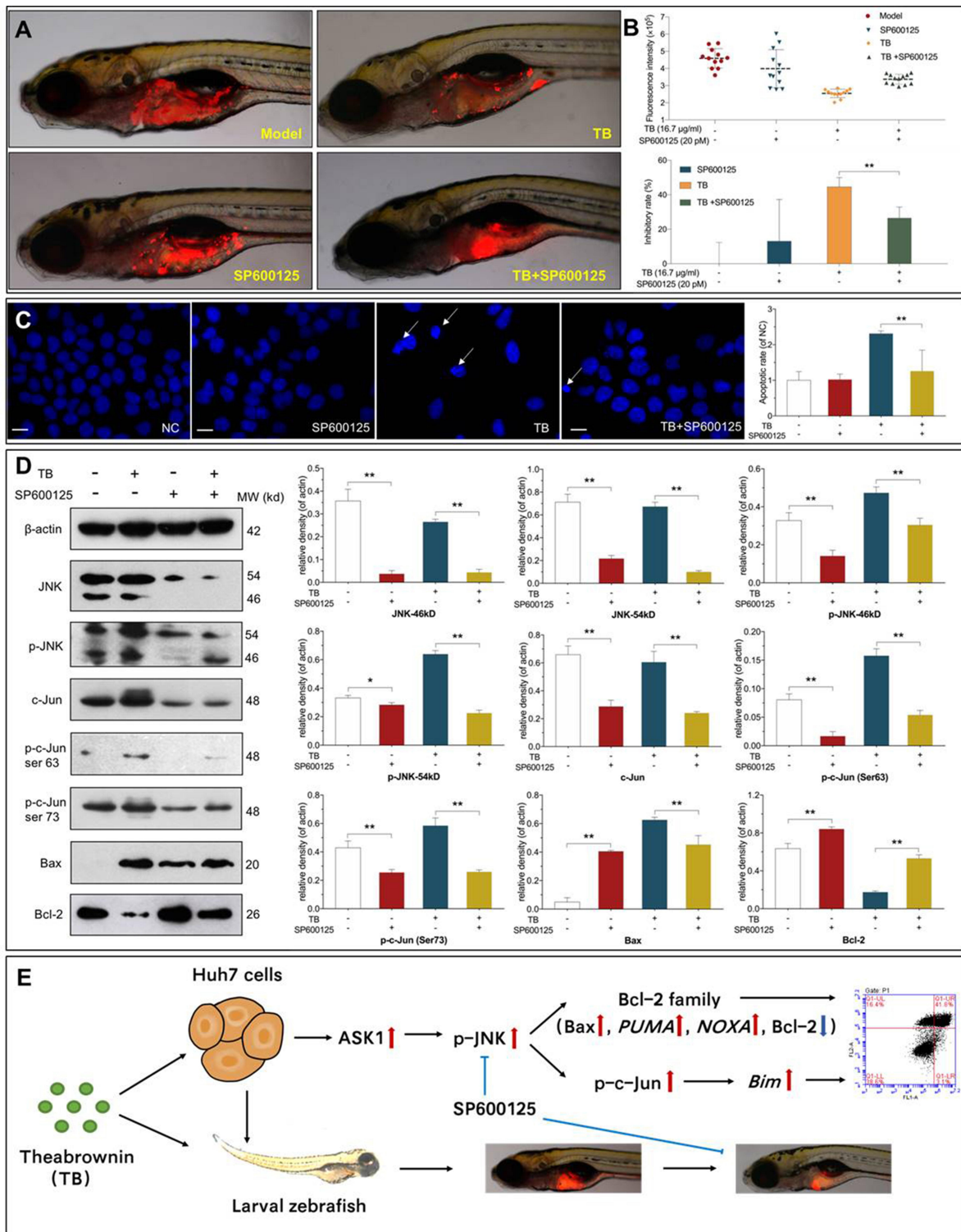


**Figure 6** (A) Observation of Huh7 xenograft zebrafishes. Zebrafishes were treated with TB (16.7 μg/mL) in the absence or presence of SP600125 (20 pM). (B) Data of fluorescence intensity and inhibitory effect of TB and SP600125. The fluorescent area (red) represents the HCC tumor mass. Values were presented as the mean ± SD (n = 30). \*\*P < 0.01. (C) Apoptotic morphology of Huh7 cells tested by DAPI staining. Cells were pretreated with 20 μM SP600125 for 1 h before treatment with or without TB (200 μg/mL). Scale bar: 50 μm. Values are presented as mean ± SD (n = 5). \*\*P < 0.01. (D) Expression and phosphorylation of the targeted proteins in Huh7 cells. Cells were pretreated with 20 μM SP600125 for 1 h before treatment with or without TB (200 μg/mL). Values are presented as mean ± SD (n = 3). \*P < 0.05; \*\*P < 0.01. (E) Overview of the effects and mechanism of TB on Huh7 cells. **Abbreviations:** TB, theabrownin; HCC, hepatocellular carcinoma; DAPI, 4',6-diamidino-2-phenylindole; NC, normal control; JNK, c-Jun N-terminal kinase; ASK-1, apoptosis signal-regulating kinase I.

inhibitory effects of TB on HCC Huh7 cells and clarified its mechanism mediated by the JNK pathway. Moreover, by using a xenograft model of larval zebrafishes, we found that TB exerted stronger tumor-inhibitory effect than that of cis-platinum. Zebrafish is a diminutive vertebrate possessing advantages as follows: 1) no immune rejection against human cells at larval stage provides more success rate for xenotransplantation; 2) body transparency of larval zebrafish provides real-time visible observation of toxicity and tumor growth; and 3) large-scale generation and rapid organogenesis provides shorter experimental period.<sup>21–23</sup> According to the previous report, the effective dose (16.7 µg/mL) of TB in the xenograft zebrafishes can be estimated as 0.75 mg/kg in human by dose conversion, which is very low and applicable in clinic.<sup>24</sup>

The in vitro data showed that TB significantly inhibited cell proliferation and induced apoptosis of Huh7 cells through activation of the JNK signaling pathway (ASK-1, JNK, p-JNK, and p-c-Jun), resulting in the overexpression of pro-apoptotic molecules (*NOXA*, *PUMA*, *Bax*, and *Bim*) (Figures 3 and 4). ASK1 is a key regulator of the intrinsic mitochondrial pathway of apoptosis and acts as an activator of the JNK pathway to respond various stresses (oxidative stress, calcium overload, inflammation, etc).<sup>25,26</sup> JNK is a multifunctional kinase in association with apoptosis, which phosphorylates c-Jun and up-regulates downstream gene expressions of *NOXA*, *PUMA*, *P21*, *Bax* and *Bim*.<sup>27</sup> C-Jun is a key regulator of cellular proliferation and apoptosis, which requires JNK-activated phosphorylation at Ser63 and Ser73.<sup>28,29</sup> *NOXA*, *PUMA*, *Bim* and *Bax* are the pro-apoptotic genes encoding Bcl-2 family members to mediate cell apoptosis.<sup>30</sup> In this study, TB activated ASK1–JNK–c-Jun signaling cascade and subsequently up-regulated the pro-apoptotic genes, resulting in apoptosis of Huh7 cells (Figure 6E). Moreover, the in vivo tumor-inhibitory and in vitro pro-apoptotic effects of TB were weakened by the JNK inhibitor SP600125, verifying that the JNK signaling mediated the anti-HCC mechanism of TB. Previously, we have reported that TB exerted anti-cancer effects on lung cancer (A549 cell line) and osteosarcoma (U2OS cell line) via the P53 signaling-dependent mechanism.<sup>16,18</sup> In this study, TB exerted significant inhibitory effects not only on P53 wild-type cell lines (HepG2 and SK-Hep-1), but also on P53-mutated cell line (Huh7). Therefore, we infer that TB's effects on P53 wild-type cancer cell lines may be dependent on the P53 signaling pathway, while that on P53-mutated cancer cell lines may be mediated by the JNK signaling pathway. Accordingly, activation of the JNK signaling

pathway can be regarded as a by-pass mechanism of TB on P53-mutated cancer cell lines, which explains the different mechanism of TB in Huh7 cells from that in other cancer cell lines (P53 wild-type).

Recently, plant-derived natural products have aroused increasing attention due to their promising effectiveness and low toxicity in prevention and treatment of HCC. Rhein is a major compound of *Cassia* species, which induces Huh7 cell apoptosis by activating ROS-dependent JNK/Jun/caspase-3 pathway.<sup>31</sup> Coronarin D as a diterpene derived from the rhizomes of *Hedychium coronarium* possesses pro-apoptotic effects on Huh7 cells via the JNK pathway.<sup>32</sup> Curcumin, a major constituent of *Curcuma longa*, is effective in suppressing proliferation, invasion, and migration of Huh7 cells through ROS-dependent JNK activation.<sup>33</sup> Therefore, the JNK signaling pathway can be regarded as a promising target for the treatment of HCC.<sup>34,35</sup> In this study, TB exerted a similar mechanism of action in comparison to the above natural products. Further investigations are needed to compare the anti-HCC efficacy between TB and other natural products.

## Conclusion

For the first time, we demonstrated that TB-induced apoptosis in Huh7 HCC cell line and inhibited tumor growth in Huh7 xenograft zebrafishes. The pro-apoptotic mechanism of TB was mediated by the JNK signaling pathway, followed by the overexpression of pro-apoptotic genes and proteins in the Bcl-2 family. Our previous studies have reported the P53 signaling-dependent mechanism of TB on many cancer cell lines.<sup>16,18</sup> Therefore, this study found a by-pass mechanism of TB on the P53-mutated cell line. Further studies are warranted to determine the effects and mechanism of TB on other cell lines with P53 mutation. To sum up, this study provides new insights into the anti-HCC efficacy of TB, contributing to the development of anti-HCC agent from natural products.

## Funding

This work was supported by National Natural Science Foundation of China (Grant No. 81774331 and 81873049), Zhejiang Provincial Natural Science Foundation of China (Grant No. LY18H270016 and LY18H270004), and Supported by Opening Project of Zhejiang Provincial Preponderant and Characteristic Subject of Key University (Traditional Chinese Pharmacology), Zhejiang Chinese Medical University (Grant No. ZYX2018006 and ZYAOXYB2019010) and

Opening Project of Zhejiang Provincial Preponderant and Characteristic Subject of Key University (Chinese Traditional Medicine), Zhejiang Chinese Medical University (Grant No. ZYXZD2019001).

## Disclosure

Jin Zhang is an employee of Theabio Co., Ltd. The authors report no other potential conflicts of interest in this work.

## References

- Torre LA, Bray F, Siegel RL, Ferlay J, Lortet-Tieulent J, Jemal A. Global cancer statistics, 2012. *CA Cancer J Clin*. 2015;65(2):87–108. doi:10.3322/caac.21262
- Jemal A, Ward EM, Johnson CJ, et al. Annual Report to the Nation on the Status of Cancer, 1975–2014, Featuring Survival. *J Natl Cancer Inst*. 2017;109(9). doi:10.1093/jnci/djx030.
- Forner A, Reig M, Bruix J. Hepatocellular carcinoma. *Lancet*. 2018;391(10127):1301–1314. doi:10.1016/S0140-6736(18)30010-2
- Sia D, Villanueva A, Friedman SL, Llovet JM. Liver Cancer Cell of Origin, Molecular Class, and Effects on Patient Prognosis. *Gastroenterology*. 2017;152(4):745–761. doi:10.1053/j.gastro.2016.11.048
- Forner A, Llovet JM, Bruix J. Hepatocellular carcinoma. *Lancet*. 2012;379(9822):1245–1255. doi:10.1016/S0140-6736(11)61347-0
- Llovet JM, Zucman-Rossi J, Pikarsky E, et al. Hepatocellular carcinoma. *Nat Rev Dis Primers*. 2016;2(1):16018. doi:10.1038/nrdp.2016.18
- Bruix J, Sherman M. Management of hepatocellular carcinoma: an update. *Hepatology*. 2011;53(3):1020–1022. doi:10.1002/hep.24199
- Bruix J, Gores GJ, Mazzaferro V. Hepatocellular carcinoma: clinical frontiers and perspectives. *Gut*. 2014;63(5):844–855. doi:10.1136/gutjnl-2013-306627
- Hu Y, Wang S, Wu X, et al. Chinese herbal medicine-derived compounds for cancer therapy: a focus on hepatocellular carcinoma. *J Ethnopharmacol*. 2013;149(3):601–612. doi:10.1016/j.jep.2013.07.030
- Huang F, Wang S, Zhao A, et al. Pu-erh Tea Regulates Fatty Acid Metabolism in Mice Under High-Fat Diet. *Front Pharmacol*. 2019;10:63. doi:10.3389/fphar.2019.00063
- Yang CS, Wang H, Sheridan ZP. Studies on prevention of obesity, metabolic syndrome, diabetes, cardiovascular diseases and cancer by tea. *J Food Drug Analysis*. 2018;26(1):1–13. doi:10.1016/j.jfda.2017.10.010
- Nakachi K, Matsuyama S, Miyake S, Suganuma M, Imai K. Preventive effects of drinking green tea on cancer and cardiovascular disease: epidemiological evidence for multiple targeting prevention. *BioFactors*. 2000;13(1–4):49–54. doi:10.1002/biof.5520130109
- Wang Q, Gong J, Chisti Y, Sirisansaneeyakul S. Production of theabrownins using a crude fungal enzyme concentrate. *J Biotechnol*. 2016;231:250–259. doi:10.1016/j.jbiotec.2016.06.010
- Xiao Y, Li M, Wu Y, Zhong K, Gao H. Structural Characteristics and Hypolipidemic Activity of Theabrownins from Dark Tea Fermented by Single Species PW-1. *Biomolecules*. 2020;10(2):204. doi:10.3390/biom10020204
- Huang F, Zheng X, Ma X, et al. Theabrownin from Pu-erh tea attenuates hypercholesterolemia via modulation of gut microbiota and bile acid metabolism. *Nat Commun*. 2019;10(1):4971. doi:10.1038/s41467-019-12896-x
- Wu F, Zhou L, Jin W, et al. Anti-Proliferative and Apoptosis-Inducing Effect of Theabrownin against Non-small Cell Lung Adenocarcinoma A549 Cells. *Front Pharmacol*. 2016;7:465. doi:10.3389/fphar.2016.00465
- Zhou L, Wu F, Jin W, et al. Theabrownin Inhibits Cell Cycle Progression and Tumor Growth of Lung Carcinoma through c-myc-Related Mechanism. *Front Pharmacol*. 2017;8:75. doi:10.3389/fphar.2017.00075
- Jin W, Zhou L, Yan B, et al. Theabrownin triggers DNA damage to suppress human osteosarcoma U2OS cells by activating p53 signaling pathway. *J Cell Mol Med*. 2018;22(9):4423–4436. doi:10.1111/jcmm.13742
- Xu Y, Wang G, Li C, et al. Pu-erh tea reduces nitric oxide levels in rats by inhibiting inducible nitric oxide synthase expression through toll-like receptor 4. *Int J Mol Sci*. 2012;13(6):7174–7185. doi:10.3390/ijms13067174
- Chen T, Peng C, Gong J, Wang Q, Zhou H. Effect of Theabrownin Extracted from Pu-erh Tea on the Metabolism of Blood Lipid in Hyperlipidemia Rats. *J Chine Inst Food Sci Tech*. 2011;11(01):20–27.
- Langheinrich U. Zebrafish: a new model on the pharmaceutical catwalk. *Bioessays*. 2003;25(9):904–912. doi:10.1002/bies.10326
- Pardo-Martin C, Chang T-Y, Koo BK, Gilleland CL, Wasserman SC, Yanik MF. High-throughput in vivo vertebrate screening. *Nat Methods*. 2010;7(8):634–636. doi:10.1038/nmeth.1481
- Konantz M, Balci TB, Hartwig UF, et al. Zebrafish xenografts as a tool for in vivo studies on human cancer. *Ann N Y Acad Sci*. 2012;1266(1):124–137. doi:10.1111/j.1749-6632.2012.06575.x
- Zhang C, Willett C, Fremgen T. Zebrafish: an animal model for toxicological studies. *Curr Protoc Toxicol*. 2003;17(1). doi:10.1002/0471140856.tx0107s17
- Pfeffer CM, Singh ATK. Apoptosis: A Target for Anticancer Therapy. *Int J Mol Sci*. 2018;19(2).
- Kim H, Oh Y, Kim K, et al. Cyclophilin A regulates JNK/p38-MAPK signaling through its physical interaction with ASK1. *Biochem Biophys Res Commun*. 2015;464(1):112–117. doi:10.1016/j.bbrc.2015.06.078
- Bogoyevitch MA, Kobe B. Uses for JNK: the many and varied substrates of the c-Jun N-terminal kinases. *Microbiol Mol Biol Rev*. 2006;70(4):1061–1095. doi:10.1128/MMBR.00025-06
- Eferl R, Wagner EF. AP-1: a double-edged sword in tumorigenesis. *Nat Rev Cancer*. 2003;3(11):859–868. doi:10.1038/nrc1209
- Behrens A, Sibilio M, Wagner EF. Amino-terminal phosphorylation of c-Jun regulates stress-induced apoptosis and cellular proliferation. *Nat Genet*. 1999;21(3):326–329. doi:10.1038/6854
- Wong RSY. Apoptosis in cancer: from pathogenesis to treatment. *J Exp Clin Cancer Res*. 2011;30(1):87. doi:10.1186/1756-9966-30-87
- Wang A, Jiang H, Liu Y, et al. Rhein induces liver cancer cells apoptosis via activating ROS-dependent JNK/Jun/caspase-3 signaling pathway. *J Cancer*. 2020;11(2):500–507. doi:10.7150/jca.30381
- Lin H-W, Hsieh M-J, Yeh C-B, Hsueh K-C, Hsieh Y-H, Yang S-F. Coronarin D induces apoptotic cell death through the JNK pathway in human hepatocellular carcinoma. *Environ Toxicol*. 2018;33(9):946–954. doi:10.1002/tox.22579
- Wang L, Han L, Tao Z, et al. The curcumin derivative WZ35 activates ROS-dependent JNK to suppress hepatocellular carcinoma metastasis. *Food Funct*. 2018;9(5):2970–2978. doi:10.1039/C8FO00314A
- Seki E, Brenner DA, Karin M. A liver full of JNK: signaling in regulation of cell function and disease pathogenesis, and clinical approaches. *Gastroenterology*. 2012;143(2):307–320. doi:10.1053/j.gastro.2012.06.004
- Wu Q, Wu W, Fu B, Shi L, Wang X, Kuca K. JNK signaling in cancer cell survival. *Med Res Rev*. 2019;39(6):2082–2104. doi:10.1002/med.21574

**OncoTargets and Therapy**

Dovepress

**Publish your work in this journal**

OncoTargets and Therapy is an international, peer-reviewed, open access journal focusing on the pathological basis of all cancers, potential targets for therapy and treatment protocols employed to improve the management of cancer patients. The journal also focuses on the impact of management programs and new therapeutic

agents and protocols on patient perspectives such as quality of life, adherence and satisfaction. The manuscript management system is completely online and includes a very quick and fair peer-review system, which is all easy to use. Visit <http://www.dovepress.com/testimonials.php> to read real quotes from published authors.

Submit your manuscript here: <https://www.dovepress.com/oncotargets-and-therapy-journal>